Interaction of ballistic particles with irregular pore walls, Knudsen diffusion, and catalytic efficiency

S. B. Santra and B. Sapoval
Laboratoire de Physique de la Matière Condensée, Ecole Polytechnique, CNRS, 91128 Palaiseau Cédex, France*
(Received 1 December 1997)

The statistical behavior of ballistic trajectories in irregular two-dimensional systems is studied numerically. The geometrical irregularity is modeled by specific prefractal shapes. Many statistical distributions arising from these trajectories are found to obey power laws of the Lévy type with an exponent of order -2. This is the case for the probability distribution of the collision numbers, collision frequencies, trajectory lengths, and free paths. The results are applied to several physical systems in which these statistics govern the physical properties. The global absorption of light by irregular, partially absorbing surfaces is found to be weakly dependent on the geometrical irregularity. In contrast, the mean interaction of a gas with an irregular surface increases strongly with the irregularity of the surface. Catalytic efficiency is also found to increase strongly with irregularity. However, surface irregularity has only weak effects on the macroscopic Knudsen diffusion. These conclusions are not modified when the partially random character of the interaction on the pore wall is taken into account. [S1063-651X(98)06706-3]

PACS number(s): 47.55.Mh, 05.60.+w, 82.65.Jv

INTRODUCTION

Ballistic trajectories are representative of several physical phenomena. They correspond to the path of light rays in reflecting irregular structures when diffraction phenomena are neglected. Ballistic trajectories also correspond to the path of atoms or molecules in confined systems or vessels at sufficiently low pressure. This is known as the Knudsen diffusion regime [1]. It determines the speed of pumping under so-called molecular or high vacuum [2]. The interaction of atoms or molecules with irregular surfaces plays a major role in heterogeneous catalysis [3,4] where porous catalysts have often very irregular surfaces down to the molecular scale. Due to the geometrical irregularity, the small scale structures of the catalyst may confine reactants and increase the interaction with the surface. Recent study of xenon nuclear magnetic resonance (Xe NMR) to probe porous structures has drawn attention to the surface interactions of rare gas atoms with solid surfaces and to their dynamics [5]. Concerning light ray trajectories, one can consider whether an irregular structure could ''trap'' light, opening the possibility to build an ''open'' blackbody. We address here the question: Does the surface geometrical irregularity play a role in these phenomena and why?

The emergence of the concept of fractal geometry has provided an efficient tool to model the influence of strong geometrical irregularity on various physical or chemical processes [6,7]. In the field of heterogeneous catalysis, the pioneering work of Avnir and co-workers [8,9] on the possible role of fractals in catalysis has triggered several studies in this direction [10]. A frequent and important physical situation occurs when the reactant pressure or the pore size is such that the reacting particles collide with the pore walls before particle-particle collisions occur. This is the Knudsen diffusion regime, where the particle paths are limited by the catalyst geometry [11].

This paper presents a numerical study of ballistic trajectories in physical or prefractal systems. By this, we mean systems of finite size (or diameter) in which the smaller feature size, the smaller cutoff, is finite. It is found that most of the quantities of interest here follow power law statistical distribution, and averages do not behave as one would generally guess intuitively [12]. For instance, the number of collisions, or the collision frequencies, are found to obey Lévy statistics, a fact already known for specular reflections in smooth pores. This is verified for both specular and random collisions on the irregular pore walls. This last property is a consequence of the partially chaotic character of the trajectories.

These power law probability distributions, for which the mean value is dominated by the so-called rare events, lead to specific unusual physical properties for each type of physical phenomenon that is considered. For example, it will be shown that the fraction of light that is reflected by such a structure is not equal to the reflection coefficient at each reflection elevated to a power equal to the mean number of collisions. In the same way, the mean collision frequency is very different from the ratio of the mean collision number to the mean duration of a trajectory.

Since Knudsen's original work [1] on molecular diffusion, several studies have been devoted to the computation of the macroscopic diffusivity and its possible dependence on geometry [13–21]. These works show that the macroscopic diffusion coefficient depends on specific averages of the paths between collisions. In most of these studies, the roughness of the surface has been ignored. On the other hand, it is known, at least empirically, that the geometrical structure of a porous catalyst may have an important influence on the catalytic efficiency [3].

The general scope of this study encompasses the statistical properties of ballistic trajectories in a model irregular structure and applications of these probabilistic results to dif-

*Unité de recherche associée du C.N.R.S. No. 1254.

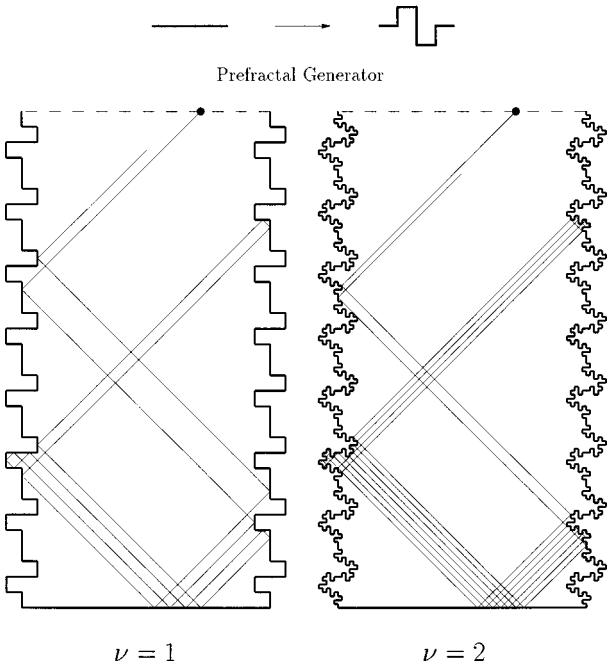

FIG. 1. Schematic representation of the first ($\nu=1$) and second ($\nu=2$) generations of the prefractal pore. The generator is shown on the top. The pore depth (128) is twice the width or diameter $W=64$, and the length of the smallest slit at $\nu=1$ is equal to 4. These values determine the computer unit length. The dotted line represents the source. Two trajectories generated by the computer code with specular reflections are shown. The pore aspect ratio is kept constant.

ferent simplified physical problems.

NUMERICAL METHOD

In our computations, only point trajectories are studied. Atoms are taken to be point mass particles and light beams are taken to have a very narrow diameter as compared to the size of the structural features. The ballistic trajectories are studied in prefractal pores built from the generator of a Koch curve of fractal dimension $D_f=3/2$. The first ($\nu=1$) and the second ($\nu=2$) pore generations are shown in Fig. 1. The ''degree of irregularity'' of the pore at any generation can be simply characterized by the ratio S of the perimeter length $L_{p,\nu}$ to $L_{p,0}$, the perimeter length of a smooth pore [22]. For our prefractal shapes, $S=2^{\nu}$. It varies from $S=1$ for the smooth pore to infinity for a mathematical fractal with $\nu \rightarrow \infty$. In the ordinary language of the studies of porous systems, the so-called specific surface of the porous catalysts (measured for instance in m^2/g) is proportional to $SL_{p,0}$.

A source of 2^{16} equally spaced particles (or rays) is fixed at the top of the pore. The smooth pore width or diameter W is chosen equal to 64 computer units and the pore depth equal to 128 computer units. The small feature size is equal to $4^{2-\nu}$. The initial incidence angle is randomly chosen from a uniform distribution of angles between 2° and 178°. A particle trajectory is described by the successive collisions. A point of collision is determined by solving the linear equations of the particle trajectory, taking into account the elements of the prefractal surface. For purely specular reflection, the reflection angle is equal to the angle of incidence. In that case, in our geometry, the reflection angle is *not* calculated from numerical computation of trigonometric functions, and the necessary reflections do not introduce numerical errors due to truncation of angle computations. This is the reason why this particular geometry, with segments parallel to the x and y axes, has been chosen. The only truncation errors come from the solution of the linear equations.

Still, because of the existence of these errors, there could appear in our calculations, besides the normal ray splitting between close trajectories hitting salient corners, trajectories that may be modified by a ''spurious'' splitting due to number truncation. To avoid spurious beam splitting, we calculate the cumulative error on the point of collision due to the numerical precision of the computer. If this error becomes greater than the distance between the point of collision and the nearest corner, we eliminate that trajectory. These ''eliminated'' trajectories are very few. Examples of specular trajectories are shown in Fig. 1.

The geometry that is used here is purely deterministic, and it is not obvious whether our computation can describe real systems. For this reason, we have also computed trajectories when the reflection on the walls is not purely specular but possesses a partial random character. In the case of light reflection, this may take into account a roughness of the individual elements building the geometrical structure. For particle-wall collision it is known that, due to the detailed nature of the microscopic interaction of an atom or a molecule with a surface, the real collision process is a complex phenomenon [23]. When the particle hits the surface, it may stay adsorbed for some time and then may desorb, exchanging momentum with the pore wall. For this reason, the particle reflection is nonspecular and presents a random character that may depend on the nature and temperature of the pore wall [23]. The random character of the trajectories may also come from the microroughness of the pore wall. In order to mimic the partial random character of each collision, the angle of reflection θ_r is related to the angle of incidence θ_i by

$$\theta_r = \theta_i + \delta\theta, \tag{1}$$

where $\delta\theta$ is a random angle distributed uniformly over a range $\pm\Gamma$. This range describes qualitatively the random character of the collisions.

The phenomena have been studied up to the fourth prefractal generation ($\nu=4$) of the pore geometry. The randomness parameter Γ is varied from 0° for specular reflection to 10° in steps of 2° for each generation. The various trajectories are indexed by the label n. For a trajectory n, we measure the successive free path lengths $l_{n,j}$ between collisions, the total trajectory length $L_n=\Sigma_j l_{n,j}$, and we count the total number of collisions N_n before the exit of the particle. In the following, $\langle\ \rangle$ indicates the average over the different trajectories n. These data are discussed and applied to different physical situations.

COLLISION NUMBER, CHAOTIC ASPECTS

The average collision number, $\langle N_n \rangle$, is given as a function of the randomness parameter Γ for different generations in Fig. 2. First and foremost, the number of collisions is found essentially independent of the randomness parameter

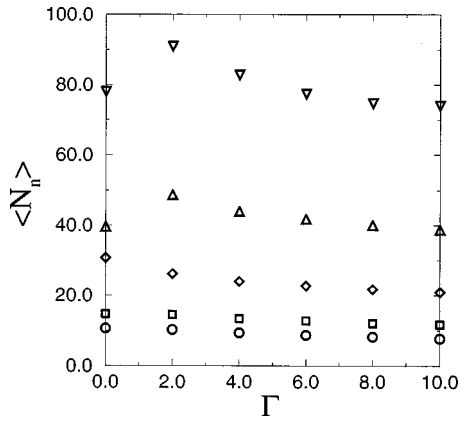

FIG. 2. Average number of collisions $\langle N_n \rangle$ vs the randomness parameter Γ for different generations. Circles: $\nu=0$ (smooth surface); squares: $\nu=1$; diamonds: $\nu=2$; up triangles: $\nu=3$; and down triangles: $\nu=4$.

Γ. Second, the average collision number increases with the irregularity.

The quasi-independence on the collision randomness is due to the irregularity in the geometry that we consider. From the point of view of chaotic systems, this geometry can be considered as giving rise to the strong sensitivity to initial conditions, which is characteristic of deterministic chaos. This is due to the existence of salient zones or angles in the structure. For example, two close trajectories may hit two different sides of a salient corner and will have very different future paths. This is shown schematically in Fig. 3.

From the point of view of the study of dynamical systems, our pores belong to the category of pseudointegrable billiards in the sense of Richens and Berry [24]. By going from one prefractal generation to the next, more and more salient corners are created, increasing the chaotic aspect of the system. It is, however, interesting to note that the statistics of the collision number are approximately the same for specular and partially random reflection. The collision number depends slightly on Γ, but the main effect is already obtained for small values of Γ. The weak effect of the randomness on the collision number has already been observed in a different geometry [25].

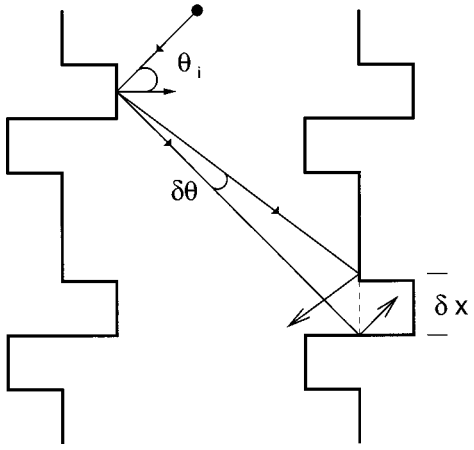

FIG. 3. Schematic illustration of the deviation of a trajectory due to a small deviation $\delta\theta$ from specular reflection.

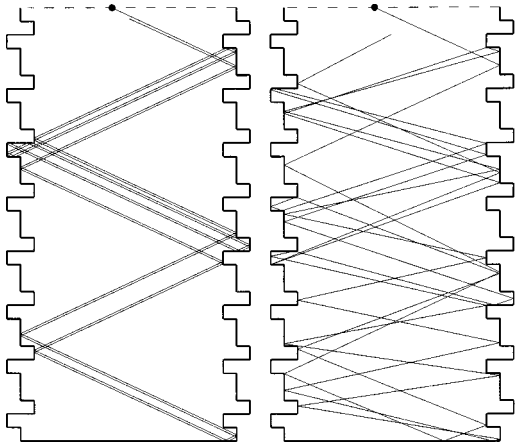

FIG. 4. Illustration of the ''chaotic'' behavior of a trajectory due to the introduction of a small randomness ($\Gamma=2°$) in the collision angle. The figure shows the sensitivity of a given trajectory to collision randomness.

This is explained schematically in Fig. 3. In the successive collisions process, the random angles do not cumulate in a linear way. The figure indicates qualitatively why a small deviation in a particular reflection can trigger a strong modification of the trajectory due to the presence of salient angles in the geometry. The deviation δx in the collision position due to the change $\delta\theta$ in the reflection angle can be estimated in the situation of Fig. 3. The deviation δx along the pore axis is of order

$$\delta x \approx \delta\theta \; l_{n,j}/\cos\,\theta_i\,, \tag{2}$$

where $l_{n,j}$ is the path length between collisions j and $j+1$. The path length $l_{n,j}$ is in this case of the order of the pore diameter (64 in our units) and the value of $\cos\,\theta_i$ can be taken of order 1/2. The change $\delta\theta$ then introduces a deviation $\delta x \sim 128\,\delta\theta$, which can be greater than the smallest slit length (4 units for the first generation) of the pore. If the deviation is greater than the slit length, it will trigger a 180° change in the trajectory direction at the next collision. This effect is more drastic for higher generations. It explains why the results are essentially insensitive to large randomness. An illustration of the sensitivity of a particular trajectory on a small randomness in the reflection angle is shown on Fig. 4. One should note that in the mathematical limit of fractality, that is when the smallest feature size goes to zero, any two close trajectories explode at the first collision.

The second result of importance is the increase of the collision number $\langle N_n \rangle$ with the irregularity. It is found to be roughly proportional to $L_{p,\nu}$, the perimeter length of the pore. This is true from one generation to the next, but it is also true for a given generation if one changes the global aspect ratio. This has been verified by changing the depth of the pore for the first generation. The increase of the collision number with irregularity suggests that an irregular surface submitted to light will be more absorbing since energy is absorbed at each reflection. This is discussed below.

NATURE OF THE COLLISION STATISTICS: THE QUESTION OF A HYPOTHETIC ''OPEN'' BLACKBODY

A blackbody is defined as an ideal body that allows *all* the incident radiation to pass into it (no reflected energy) and

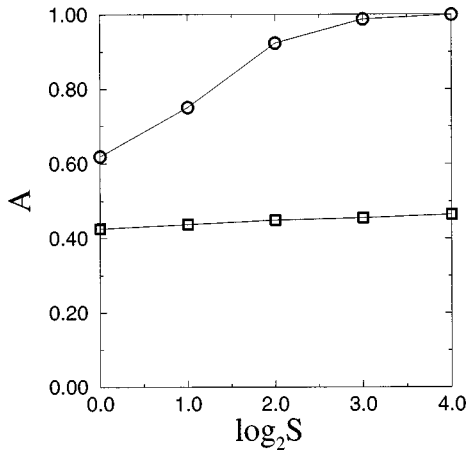

FIG. 5. Computed absorption coefficient for a surface reflection coefficient $r=0.9$. The circles represent an absorption estimated from the average collision numbers using Eq. (3), and the squares represent the effective absorption computed using Eq. (4).

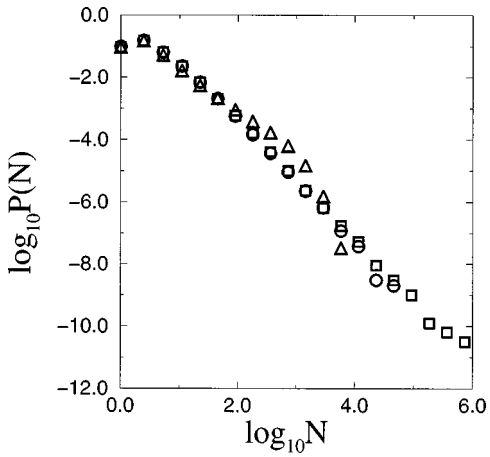

FIG. 6. Probability distribution $P(N)$ of the collision number N. The $P(N)$ values for several systems are shown. Circles are for $\nu=3$ and $\Gamma=0°$; squares are for $\nu=4$ and $\Gamma=0°$; and triangles are for $\nu=4$ and $\Gamma=2°$.

absorbs internally *all* the incident radiation (no transmitted energy) [26,27]. Physically it is built as a closed cavity with a small hole such that any light ray that enters the cavity is reflected a sufficient number of times to be totally absorbed. It is known that the roughness of a surface can have profound effects on the radiative properties and will indeed become a controlling factor when the roughness is large in comparison with the wavelength of the radiation being considered [27].

We address here the following question: suppose light is reflected by the prefractal irregular surface in such a way that light rays undergo many reflections before being finally reflected from the system. One could guess intuitively that, because of the irregular structure of the reflecting geometry shown in Fig. 1, the number of reflections will be increased, increasing the system absorbing power. If this were true, the system would behave as an ''open'' blackbody, which could have practical applications. If the reflection coefficient r is supposed for simplicity to be isotropic, a rough estimation of the effective absorption would be

$$A_{\text{est}}=1-r^{\langle N\rangle}, \tag{3}$$

where $\langle N\rangle$ is the mean number of collisions.

One of our main results is that this estimate is grossly wrong. Indeed, the fraction of energy really absorbed is given by

$$A=1-(1/N_{\text{tr}})\sum_{n} r^{N_n}, \tag{4}$$

where N_{tr} is the total number of trajectories that have been computed.

The result of the calculation of expressions (3) and (4) is given in Fig. 5. A strong discrepancy between the two values is observed. This shows that the intuitive guess expressed by Eq. (3) is wrong. Indeed, this particular geometry increases the absorbing power, but not to the extent that is guessed from Eq. (3). The effect is only partial and does not, for this particular geometry, justify the idea of an ''open'' blackbody.

The reason for this discrepancy lies in the particular statistics of the number of reflections. Although it is true that the *mean* number of collisions is strongly increased by the irregularity, this statistical mean is dominated by a few rays that see a very large number of reflections. In other words, most of the light rays see only a moderate increase in the number of reflections, and consequently, the effect of the irregularity on the global absorption is weak.

The knowledge of the probability distribution of the reflection number helps one to understand this behavior. The probability $P(N)$ to have N collisions is shown in Fig. 6. The distribution of N appears to be essentially independent of ν and Γ. Secondly, the tail of the distribution is a power law with an exponent -1.98, approximately equal to -2. This is a Lévy-type distribution [12], which has in principle no second moment in the limit $N\to\infty$. In the same limit, the first moment of the distribution

$$\langle N_n\rangle=\int NP(N)dN \tag{5}$$

diverges logarithmically. This means that the majority of the rays has a small number of reflections, but the average number of reflections is dominated by the few rays that undergo a large number of collisions. In such a case, the usual arithmetic average is not representative of the phenomenon.

One should recall that the irregularity is not the cause for a Lévy-type power law [17]. For example, it is easy to show that the probability $P(N)$ of the collision number for specular reflections in a smooth pore ($\nu=0$) is a power law of exponent -2. In this case the number of collisions $N(\theta)$ for an angle of incidence θ is given by $N(\theta)=C/\tan(\theta)$ where $C\approx 2L_{p,0}/W$. The factor 2 comes from the fact that our pore is closed at the bottom. For specular reflections this is equivalent to an open pore of double length. For θ uniformly distributed between 0 and π, this leads to $P(N)=\pi^{-1}|d\theta/dN|=\pi^{-1}C/(C^2+N^2)\propto N^{-2}$ for $N\gg C$. This is why there is already a large difference between the global absorption coefficients calculated from Eqs. (3) and (4) for $\nu=0$.

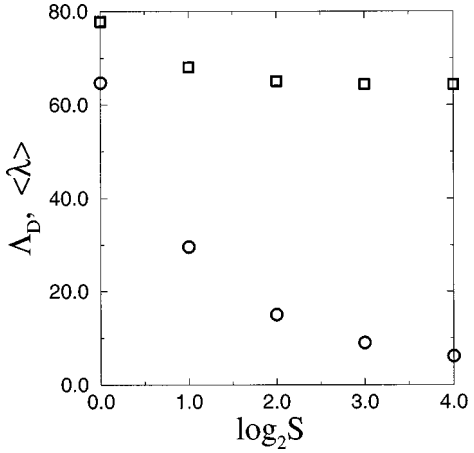

FIG. 7. Knudsen diffusivity: dependence of $\langle\lambda\rangle$ (circles) and Λ_D (squares) on the irregularity (computer units). The diffusivity, proportional to Λ_D, is found to be nearly independent of the pore irregularity.

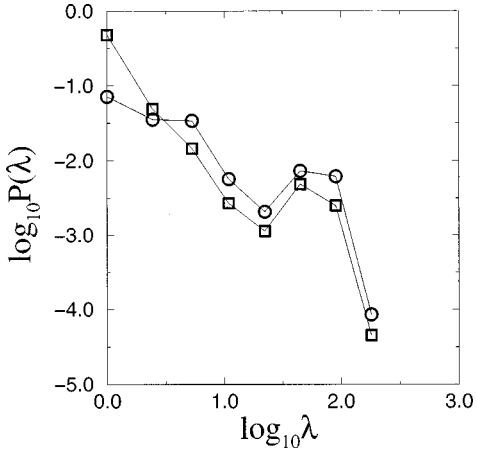

FIG. 8. Probability distribution $P(\lambda)$ of the individual mean free paths λ (computer units) for generations $\nu=1$ (circles) and $\nu=2$, (squares). The relative number of small paths increases rapidly with the irregularity. The hump in the distribution corresponds to path lengths of the order of the pore diameter, here 64.

The median value of the collision number, which measures the number of reflections of the majority of the rays, is of more use here. It is found of order 4 to 8 for our geometries. If one uses the median value in Eq. (3), the agreement is much better.

One should note that, from the data in Fig. 6, it seems that for specular reflection, the maximum number of collisions is larger than in the case of partial randomness in the collision process. This may be due to a geometrical resonance that could be blurred by the random character of the collisions. Ascertaining this fact would require extremely large simulations, which are beyond the scope of this paper.

It should also be noted that the results on the collision number and distribution cannot be extended from two to three-dimensional trajectories. The number of collisions is increased by going to three dimensions but the role of a geometrical irregularity is unknown. The possibility of a real open blackbody in three dimensions remains unanswered.

KNUDSEN DIFFUSIVITY

To calculate the macroscopic diffusivity D, we use the expression given by Derjaguin [12] for a pore network in three dimensions

$$D=(c/6\langle\lambda\rangle)\left\langle \boldsymbol{l}_{n,1}\cdot\boldsymbol{l}_{n,1}+2\sum_{j=2\rightarrow\infty}\boldsymbol{l}_{n,1}\cdot\boldsymbol{l}_{n,j}\right\rangle, \tag{6}$$

where c is the average velocity and $\langle\lambda\rangle$ the usual arithmetic average of the free path between collisions $|\boldsymbol{l}_{n,j}|$. Assuming that the consecutive paths are mutually independent, Derjaguin's formula simplifies to

$$D=(c/4)\langle\lambda^2\rangle/\langle\lambda\rangle \tag{7}$$

in two dimensions. Here $\langle\lambda^2\rangle$ is the average of the square of the individual free paths $|\boldsymbol{l}_{n,i}|^2$ or mean square displacement. There exists then in this problem an ''equivalent diffusion path'' defined by $\Lambda_D=\langle\lambda^2\rangle/\langle\lambda\rangle$ such that $D=c\Lambda_D/4$. The dependence of $\langle\lambda\rangle$ and Λ_D on the irregularity S is given in Fig. 7.

The result is striking: although the ordinary mean free path $\langle\lambda\rangle$ decreases with S and seems to saturate, the diffusivity proportional to $\Lambda_D=\langle\lambda^2\rangle/\langle\lambda\rangle$, is essentially independent of the irregularity. The length Λ_D is found of the order of the pore diameter, here equal to 64, independently of the collision randomness and the irregularity. To understand this fact, it is useful to consider the probability distribution $P(\lambda)$ of the individual free paths of length λ, which is shown in Fig. 8. The first observation is that the distribution corresponds approximately to Lévy *flights* with an upper cutoff of the order of the pore size. Secondly, the relative number of short free paths increases enormously when the irregularity is increased. This is to be contrasted with the case of the smooth pore. In this case $\lambda=W/\cos(\theta)$ and, as $P(\lambda)d\lambda=\pi^{-1}d\theta$, one can write

$$P(\lambda)=\pi^{-1}(W/\lambda^2)(1-W^2/\lambda^2)^{-1/2} \tag{8}$$

of order $\pi^{-1}(W/\lambda^2)$ for $\lambda\gg W$. The existence of a Lévy distribution for paths much smaller than the pore width is a specific consequence of the pore irregularity.

These values, however, do not contribute significantly to the averages $\langle\lambda\rangle$ and $\langle\lambda^2\rangle$. One can write

$$\langle\lambda\rangle=\int\lambda P(\lambda)d\lambda, \tag{9}$$

$$\langle\lambda^2\rangle=\int\lambda^2 P(\lambda)d\lambda. \tag{10}$$

The integrands of these integrals are shown in Fig. 9. It is clear that the integrals (9) and (10) take their values for values of λ of the order of the pore width. It can be seen in Fig. 8 that this is also true for the next higher generation. This explains why the Knudsen diffusivity is only weakly modified in our structures. One should note that our structures are smooth on large scales. They represent a surface irregularity in which the largest irregular feature is kept smaller than the pore diameter. This is why our results differ from those obtained by Coppens for structures irregular at all scales [21].

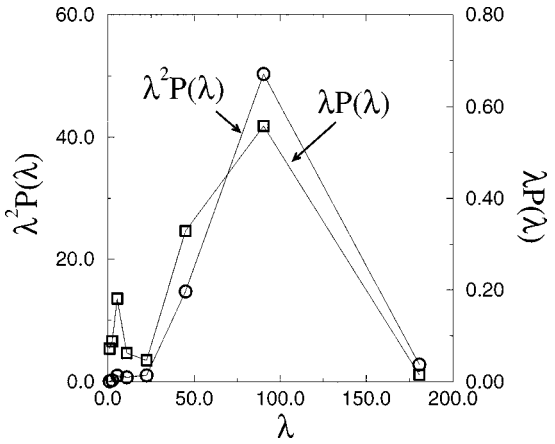

FIG. 9. Distribution of the integrands $\lambda P(\lambda)$ (squares) and $\lambda^2 P(\lambda)$ (circles) in Eq. (9) and (10) for a pore of the first generation. Lengths are expressed in computer units defined in Fig. 1. One observes that the integrals of these functions take their main contributions from the same values of the free paths, which are of the order of the pore diameter.

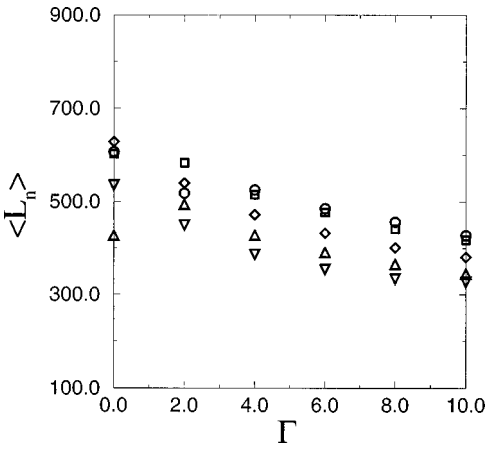

FIG. 10. Dependence of the average length of the trajectories $\langle L_n \rangle$ on Γ for different generations (computer units). Same symbols as in Fig. 2. The length $\langle L_n \rangle$ also measures the average trajectory duration $\langle T_n \rangle$ if the velocity is equal to 1.

MEAN INTERACTION BETWEEN PARTICLES AND IRREGULAR PORE WALLS

We address now the following question: suppose that we consider a gaseous system at sufficiently low pressure for collisions between particles to be negligible as compared to collisions with the pore walls. Suppose that the particles, for instance xenon atoms, are absorbed at each collision for a short duration τ. During this time the nuclear magnetic resonance of the isotope ^{129}Xe (spin 1/2) is submitted to a small shift in frequency [5,28,29]. What is the average interaction, or average NMR shift? This shift $\Delta\omega$ will be proportional to the fraction of the time during which the nuclei are in interaction with the surface or simply to the frequency of the collisions, if the residence time is short enough. We assume that we are in this situation.

To compute the mean interaction, we need to consider a steady state in which the pressure is constant. If all the trajectories are initiated simultaneously at the entrance of the pore, the simple average over the trajectories does not represent a system at constant pressure, because the duration of the various trajectories is different. Some particles are reflected out of the system very quickly, while others spend a longer time in the pore. In order to mimic a constant pressure, we need to replace the particles as soon as they leave the system. A trajectory n of duration T_n is then renewed $1/T_n$ times during the unit time, and the number of collisions per unit time is equal to $F_n = N_n / T_n$. To see the effect of the randomness and the irregularity on the average interaction at *constant pressure*, one has to estimate the average of the frequencies over the various trajectories. This is a way to restitute an ensemble average from our numerical results on the statistics of the trajectories. One needs to measure the total time T_n spent by the trajectory n in the pore. This time can be calculated from the trajectory length L_n, since $T_n = L_n / c$, where c is the average velocity of the particle. The measured dependence of the average trajectory length $\langle L_n \rangle$ on S and Γ is given in Fig. 10. It is found that the average trajectory length is of the order of a few pore depths, almost independently of Γ and ν. One should, however, note that these lengths are extremely dispersed, as indicated by Fig. 11, which gives the probability distribution of the lengths, or durations, of the different trajectories. Note that in the case of a smooth pore there exists no trajectory of length smaller than $L_{p,0}$ here equal to 256. The existence of trajectories of small length or durations is then a specific consequence of the geometrical irregularity.

Since the average collision number increases with the irregularity with nearly constant average duration, the average collision frequency should also increase. The collision frequency $F_n = N_n / T_n$ is directly related to the arithmetic average λ_n of the free paths along the trajectory n, since by definition, $\lambda_n = L_n / N_n = c T_n / N_n$. The average frequency is then proportional to the inverse of this mean free path

$$\langle F_n \rangle = \langle N_n / T_n \rangle = c \langle 1/\lambda_n \rangle. \tag{11}$$

The mean interaction is then related to the *harmonic mean* of the *arithmetic* mean free path *along the n trajectory*. The simulation results are given in Fig. 12. They indicate that the average collision frequency increases rapidly with S, the ir-

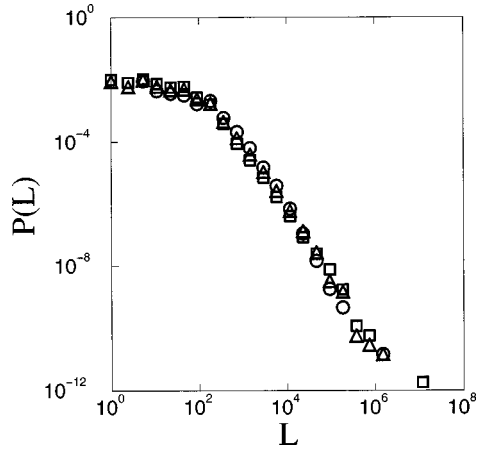

FIG. 11. Probability distribution $P(L)$ of the total lengths L or durations of the trajectories for specular reflections (computer units). Different symbols correspond to the different generations of the pore: circles for $\nu=1$, triangles for $\nu=2$, and boxes for $\nu=3$. The tail of the distribution is of the Lévy type.

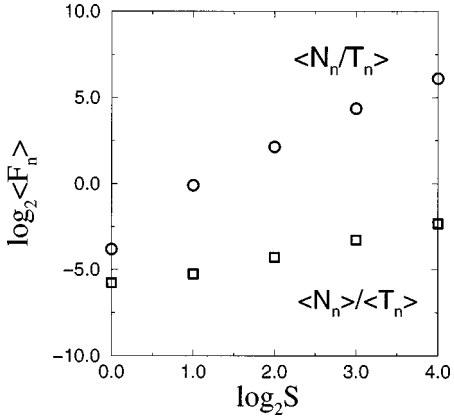

FIG. 12. Dependence of the average interaction or average collision frequency $\langle F_n \rangle$ on the irregularity S. Note that the average frequency is very different from the ratio of the averages $\langle N_n \rangle / \langle T_n \rangle$.

regularity of the pore. One should also note that the average $\langle N_n / T_n \rangle$ of the ratio N_n / T_n is much larger than the ratio of the averages $\langle N_n \rangle / \langle T_n \rangle$.

To understand why the irregularity plays such a role, one has to discuss the probability distribution $P(F)$ of the collision frequencies. It is shown in Fig. 13. It is also a Lévy distribution of exponent of order -2. But, as $\lambda_n = L_n / N_n = c T_n / N_n = c / F_n$, if one knows $P(F)$ one can retrieve the probability distribution of λ_n by the relation $P(F) = P(\lambda_n) |d\lambda_n / dF|$. Then as $P(F) \sim F^{-2}$,

$$P(\lambda_n) \sim F^{-2} |d\lambda_n / dF| \sim \lambda_n^2 \lambda_n^{-2} \sim \text{const.} \qquad (12)$$

The distribution (over the different trajectories) of the arithmetic mean free path λ_n should then be approximately *uniform*. This is an unexpected result: there exists also a large dispersion of the *arithmetic mean free path along a trajectory*. The statistics of the lengths λ_n, obtained directly from the simulations, are shown in Fig. 14. The approximation $P(\lambda_n) \approx$ constant is indeed verified for all the small values of λ_n. The mean frequency $\langle F_n \rangle$ is now given by

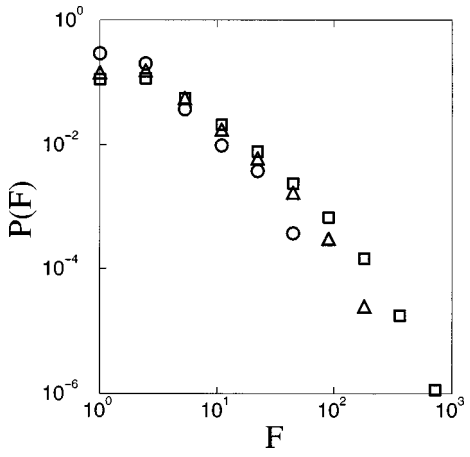

FIG. 13. Probability distribution $P(F)$ of the collision frequency F. Different symbols correspond to the different generations of the pore: circles for $\nu = 1$, triangles for $\nu = 2$, and squares for $\nu = 3$. Those distributions are obtained for specular reflections and are found to be of the Lévy type.

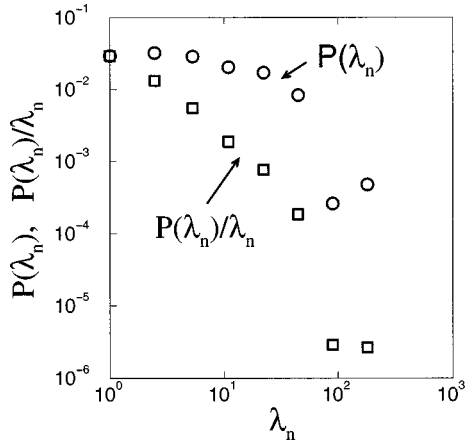

FIG. 14. The circles represent the distribution $P(\lambda_n)$ of the arithmetic mean free path λ_n along the nth trajectory for the second generation of the pore (computer units). The squares represent the distribution of $P(\lambda_n)/\lambda_n$, which is the integrand for the average collision frequency expressed by Eq. (13).

$$\langle F_n \rangle = \int F P(F) dF = c \int (1/\lambda_n) P(\lambda_n) d\lambda_n . \qquad (13)$$

As $P(\lambda_n)$ is essentially independent of λ_n, the value of this integral is dominated by the *small* values of mean free path λ_n, as shown by Fig. 14 where $(1/\lambda_n) P(\lambda_n)$ is also shown. If $P(\lambda_n) \approx$ const, the value of the integral is of the order of const$\times (\lambda_{n,\min})^2$, where $\lambda_{n,\min}$ is the minimum between these mean free paths. Here again, the properties of the system are governed by the rare trajectories in which the *arithmetic* mean free path is small. These trajectories dominate the average interaction with the pore walls. Here again, this is a specific effect of the irregular structure as in a smooth pore the smaller free path is equal to the pore width.

The results given in Fig. 11 suggest a specific behavior for the pumping speed in the Knudsen regime. The probability distribution of the trajectories duration indicates that, for a long time, the remaining pressure should drop as a power law of time.

CATALYTIC EFFICIENCY

Since the average collision frequency increases with the irregularity, one can expect that the efficiency of a porous catalyst will increase with the irregularity. We consider first the simple reaction, $A \rightarrow A^*$ (products) on collision with the pore wall. There exist two reasons why irregular catalysts are more efficient. First, there is an increase in the total surface, described here by the factor S. Second, there could exist a specific increase of the catalyst yield *per unit length* of the wall if, for a given perimeter, the irregularity increases the probability of collisions with the wall. For this reason, we define the specific catalytic efficiency η as the number of catalytic reaction events that takes place per unit length (or equivalently per catalytic site) per unit time [3].

The catalyst efficiency is then, apart from constant factors, the number of products A^* created per unit time *in*

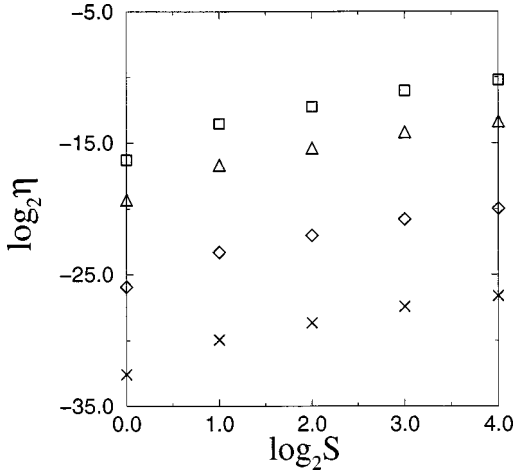

FIG. 15. Dependence of the specific catalytic efficiency η on the irregularity S for different reaction probabilities corresponding to $N_0=10$ (squares), $N_0=10^2$ (triangles), $N_0=10^4$ (diamonds), $N_0=10^6$ (crosses). The efficiency increases with S for any value of the reaction probability.

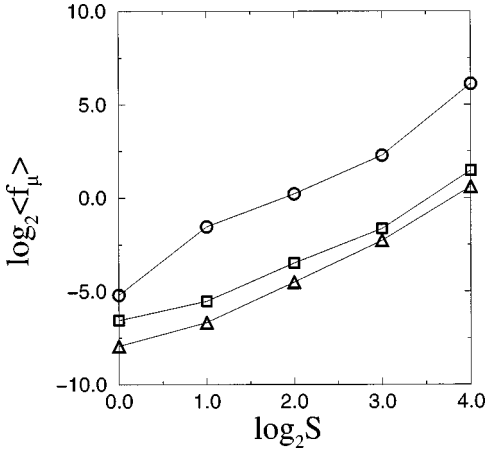

FIG. 16. Dependence of the average collision frequency up to μ collisions $\langle f_\mu \rangle$ on the irregularity S. Different symbols correspond to $\mu=2$ (circles), $\mu=10$ (squares), $\mu=90$ (triangles). The collision frequencies increase with the irregularity.

steady state. The steady state is a situation where the pressure of A at the pore entrance is constant. Here, it means that each time one A^* product is obtained, an A must be renewed at the pore entrance. We must then compute first the global production *frequency* over one trajectory, then average over all trajectories. To find this quantity, we must take care that the catalytic event itself is a random process. The catalytic process is characterized by the mean number $N_0 \gg 1$ of collisions necessary for an individual reaction $A \rightarrow A^*$ to occur. The quantity $1/N_0$ is the reaction probability per collision. With such a constraint, the probability P_μ that the reaction occurs exactly at the μ_{th} collision on the wall is equal to

$$P_\mu = (1/N_0)\exp(-\mu/N_0). \tag{14}$$

In that case, the specific efficiency along a trajectory n can be written as

$$\eta_n = \{1/L_{p,\nu}\} \sum_\mu (P_\mu / T_{\mu,n}), \tag{15}$$

where $T_{\mu,n}$ is the time spent by the particle in the trajectory n to reach μ collisions. The global catalyst efficiency is $\eta = \langle \eta_n \rangle$. The simulation results for η are given in Fig. 15. They indicate that the efficiency increases with S for any value of the number N_0 of collisions required to obtain a product. This means that a porous catalyst's efficiency depends strongly on its small scale irregularity. It is important to note that the increase in the efficiency is independent on N_0. This is only possible if not only the average frequency, but also the collision frequency up to any collision number increases with the irregularity. In Fig. 16, we have plotted the average $\langle f_\mu \rangle$ of the collision frequency $f_{\mu,n}=\mu/T_{\mu,n}$ ''up to μ collisions.'' It can be seen that $\langle f_\mu \rangle$ increases with the irregularity for any value of μ. This indicates that when one goes from one generation to the next, the addition of small scale structures increases the collision frequency for most of the trajectories. When the reaction probability is very small, such that N_0 is larger than any μ that belongs to the trajectories, the value of P_μ is constant and equal to $(1/N_0)$, and $\eta = \langle \eta_n \rangle = \{1/L_{p,\nu}\}\langle F_n \rangle / N_0$. The specific efficiency then reproduces the average frequency, given in Fig. 12, divided by the perimeter length.

These results also throw new light on the phenomenon of catalyst poisoning. We consider the case where the barrier energy for a poisonous species B to be trapped from the gas phase on an active site is large. In that case, most of the poisonous species are reflected when hitting the surface. (In that situation it is possible that the barrier for desorption is even larger so that the poisonous species is strongly bonded once when it has been trapped). In the situation of a dilute poisonous gas, it will be trapped extremely slowly by the catalyst because the effective rate of trapping is the product of two small probabilities. Not only the elementary probability for an individual B to be absorbed on a catalytic center may be small but also the probability for the diluted B to follow one of those rare trajectories with large N is also small. From this qualitative point of view, the catalyst's efficiency and the poisoning effects may be due to the same rare trajectories.

SUMMARY

The statistical properties of ballistic trajectories have been studied in two-dimensional irregular porous structures. The probability distribution for the collision numbers, the collision frequencies, trajectory durations or lengths, and the free paths between collisions are described by Lévy distributions with exponent nearly equal to -2. The irregularity induces a majority of path lengths smaller than the pore width and several physical properties have been found to be governed by the existence of small scale structures in the system geometry.

The catalytic efficiency in the Knudsen diffusion regime is found to increase rapidly with the geometrical irregularity of prefractal pores. In the same regime, the macroscopic diffusivity is not modified by the surface roughness.

These results have been obtained for two-dimensional porous systems and the study should be extended to the third dimension. If the same properties arise in three-dimensional systems, they could have great practical significance, be-

cause they show that the catalytic efficiency is controlled by the geometrical irregularity of a porous system independently of the macroscopic transport in the medium.

The fact that the essential results do not depend on the random character of the reflection is an example that the study of deterministic fractals permits one to grasp some of the essential properties of strong geometrical disorder [7].

ACKNOWLEDGMENTS

We gratefully acknowledge helpful discussions with P. Pfeifer, M. O. Coppens, P. Lévitz, and B. B. Mandelbrot. The authors thank Dr. Lévitz for communicating his results prior to publication. The computation has been performed at the IDRIS, Orsay, France.

[1] M. Knudsen, Ann. Phys. (N.Y.) **28**, 75 (1909).
[2] S. Dushmann, *Scientific Foundations of Vacuum Technique* (John Wiley and Sons, New York, 1962)
[3] J. M. Thomas and W. J. Thomas, *Principles and Practice of Heterogeneous Catalysis* (VCH, Weinheim, 1997), and references therein.
[4] G. F. Froment and K. B. Bischoff, *Chemical Reactor Analysis and Design* (John Wiley and Sons, New York, 1990), and references therein.
[5] V. Pasquier, P. Lévitz, and A. Delville, J. Phys. Chem. **100**, 10 249 (1996), and references therein.
[6] B. B. Mandelbrot, *The Fractal Geometry of Nature* (Freeman, San Francisco, 1982).
[7] B. Sapoval, *Fractals* (Aditech, Paris, 1989); *Universalités et Fractales* (Flammarion, Paris, 1997).
[8] D. Avnir, D. Farin, and P. Pfeifer, J. Chem. Phys. **79**, 3566 (1983); Nature (London) **308**, 261 (1984).
[9] P. Pfeifer and D. Avnir, J. Chem. Phys. **79**, 3558 (1983).
[10] R. Kopelmann, in *The Fractal Approach to Heterogeneous Chemistry*, edited by D. Avnir (Wiley, New York, 1989), p. 295, and references therein.
[11] Usual diffusion, in which the mean free path is much smaller than the pore size, towards irregular surfaces and its role in heterogeneous catalysis are discussed in B. Sapoval, in *Fractals and Disordered Systems*, 2nd ed., edited by A. Bunde and S. Havlin (Springer-Verlag, Berlin, 1996), p. 232; and P. Pfeifer and B. Sapoval, in *Dynamics in Small Confining Systems II*, edited by J. M. Drake *et al.*, MRS Symp. Proc. No. 366 (Materials Research Society, Pittsburgh, 1995), p. 271.
[12] See for instance J. Klafter, M. F. Shlesinger, and G. Zumofen, Phys. Today **49**, 33 (1996) and references therein.
[13] B. Derjaguin, C. R. (Dokl.) Acad. Sci. URSS **7**, 623 (1948).
[14] J. W. Evans, M. H. Abbasi, and A. Sarin, J. Chem. Phys. **72**, 2967 (1980).
[15] Y. Nakano and J. W. Evans, J. Chem. Phys. **78**, 2568 (1983).
[16] P. Lévitz, in *Dynamics in Small Confining Systems*, edited by J. M. Drake *et al.*, MRS Symp. Proc. No. 290 (Materials Research Society, Pittsburgh, 1993), p. 197.
[17] P. Lévitz, J. Phys. Chem. **97**, 3813 (1993).
[18] P. Lévitz, Europhys. Lett. **39**, 6 (1997).
[19] M. O. Coppens and G. F. Froment, Chem. Eng. Sci. **49**, 4897 (1994).
[20] M. O. Coppens and G. F. Froment, Chem. Eng. Sci. **50**, 1207 (1995).
[21] M. O. Coppens, Fractals **3**, 807 (1995); and in *Fractals in Engineering: From Theory to Industrial Applications*, edited by J. Lévy-Vehel, E. Lutton, and C. Tricot (Springer, London, 1997), p. 336.
[22] R. P. Wool and J. M. Long, Macromolecules **26**, 5227 (1993); and R. P. Wool, *Structure and Strength of Polymer Interfaces* (Hanser, City, 1994).
[23] J. P. Valleau, D. J. Diestler, M. Schoen, A. W. Hertzner, and M. E. Riley, J. Chem. Phys. **95**, 6194 (1991), and references therein.
[24] P. J. Richens and M. V. Berry, Physica D **2**, 495 (1981).
[25] S. B. Santra, B. Sapoval, and O. Haeberlé, in *Fractals in Engineering: From Theory to Industrial Applications*, edited by J. Lévy-Vehel, E. Lutton, and C. Tricot (Springer, London, 1997), p. 350.
[26] G. A. Rutgers, in *Encyclopedia of Physics*, edited by S. Flügge, Light and Matter II Volume XXVI (Springer-Verlag, Heidelberg, 1958), p. 138.
[27] R. Siegel and J. R. Howell, *Thermal Radiation and Transfer* (McGraw-Hill Kogakusha, Ltd. Tokyo, 1972).
[28] C. Dybowski, N. Bansal, and T. M. Duncan, Annu. Rev. Phys. Chem. **42**, 433 (1991).
[29] J. Fraissard, in *Encyclopedia of Nuclear Magnetic Resonance*, edited by D. M. Grant and R. K. Harris (John Wiley and Sons, New York, 1990), p. 3058.